



A robust clustering algorithm using spatial fuzzy C-means for brain MR images

Madallah Alruwaili*, Muhammad Hameed Siddiqi, Muhammad Arshad Javed

College of Computer and Information Sciences, Jouf University, Sakaka, Saudi Arabia

ARTICLE INFO

Article history:

Received 29 July 2019

Revised 19 September 2019

Accepted 21 October 2019

Available online 18 November 2019

Keywords:

Clustering algorithm

MRI

Fuzzy C-means

ABSTRACT

Magnetic Resonance Imaging (MRI) is a medical imaging modality that is commonly employed for the analysis of different diseases. However, these images come with several problems such as noise and other imaging artifacts added during acquisition process. The researchers have actual challenges for segmentation under the consideration of these effects. In medical images, a well-known clustering approach like Fuzzy C-Means widely used for segmentation. The performance of FCM algorithm is fast in noise-free images; however, this method did not consider the spatial context of the image due to which its performance suffers when images corrupted with noise and other imaging relics. In this paper, a weighted spatial Fuzzy C-Means (wsFCM) segmentation method is proposed that considered the spatial information of image. Moreover, a spatial function is also developed that integrate a membership function. In order assess this function, a neighborhood window is established around a pixel and more weights have been assigned to those pixels which have greater correlation with central pixel in local neighborhood. By integration of this spatial function in membership function, the modified membership function strengthens the original membership function in handling the noise and intensity inhomogeneity, which has the ability to preserves and maintains structural information like edges. A comprehensive set of experimentation is performed on publicly accessible simulated and real standard brain MRI datasets. The performance of the proposed method has been compared with existing state-of-the-art methods. The results show that the performance of the proposed method is better and robust in handling noise and intensity inhomogeneity than of the existing works.

© 2019 Production and hosting by Elsevier B.V. on behalf of Faculty of Computers and Information, Cairo University. This is an open access article under the CC BY-NC-ND license (<http://creativecommons.org/licenses/by-nc-nd/4.0/>).

1. Introduction

Medical imaging is positioning itself towards automation and intelligence in the second decade of 21st century. Magnetic resonance imaging (MRI) is a noninvasive medical imaging method for producing anatomical structures of the human body [1]. This is one of the common and widely used imaging techniques in medical imaging due to its excellent capability for soft tissue imaging. This technique has gained appreciable penetration in medical

imaging during last few years due to its safety, reliability and efficiency features. MRI is most often used for the diagnosis and detection of tumors, lesions, to observe tissues growth, treatment planning and other abnormalities in brain soft tissues. The MRI method creates scans from measured signals that come directly from the object without needs to inject contrast agents. There is no problem regarding the radiation as it works in the radio frequency range. Lastly, it creates different images concentrating on one specific property of a same object by changing some intrinsic parameters of the system. This technique has a problem that is related to application of magnetic fields in the encoding process. These images are subject to different noises while taking the data, which affects quality and diagnostics of the image. Investigating MRI images help the doctors to take right judgments. Nevertheless, MRI noises reduce the quality of the image that badly disturbs the work of analyzing and processing image, for instance registration, classification, segmentation, and visualization. To achieve consistent examination results, eliminating the noise from the MRI image is necessary before conducting image processing [2].

* Corresponding author.

E-mail addresses: madallah@ju.edu.sa (M. Alruwaili), mhsiddiqi@ju.edu.sa (M.H. Siddiqi), arsh_qau@ju.edu.sa (M.A. Javed).

Peer review under responsibility of Faculty of Computers and Information, Cairo University.



Production and hosting by Elsevier

The image segmentation in a divider contains diverse sections that transmit alike pixels inside same sections and unlike from another sections pixels. Image segmentation plays a vital role in medical imaging. In MRI images examination, the segmentation is widely used to calculate and imagine the functional constructions of brain, for examining variations in brain, for defining compulsive sections, and for medical preparation and image-guided involvements [3]. MRI scanners produce many images for patient area of interest and thus a doctor (radiologist) has to assess qualitatively a huge amount of MRI images of a distinct patient produced by MRI scanners. Despite their best expertise and effort, human judgment and sight can be often deceiving. The incorrect judgment might cause harm consequences [4]. Automated support in disease diagnosis and detection process can not only improve the judgment quality but also ease the tedious process of diagnosis. This is particularly true with MRI based diagnosis of brain diseases because of unique intricate structure of brain as well as the significance of extremely precise detection. In such a scenario, automatic intelligent segmentation technique of brain classes tissue is needed to finish the segmentation of MR images. However, this brain tissue segmentation is a very concerning task because of the morphology of brain tissue structure joint with noise, incomplete capacity consequence and image preference field existing the separation of their association with robust pixel uncertainty and indecision [5,6]. This level of complexity clearly points towards a need for such computer method, which could reproduce accurate segmentation under these challenges and provide support to radiologists or experts or medical community in decision making. There are 86 billion (approx) nerve cells or neurons and billions of nerve fibers or axons in brain, which are known as gray matters (GM) and white matters (WM) respectively. These neurons are connected by trillions of connections, or synapses [7]. The brain also carries in it an amount of cerebrospinal fluid (CSF) which has some concentrated amount of energy supplement of glucose, salts, and biological ingredients of enzymes, and white blood cells. In numerous clinical applications, the correct segmentation of brain MR images in certain brain tissue classes is a significant concern, which might be varied such as WM, GM and CSF is a crucial job [8]. If this information is in hand, then the quick analysis might be done. For disease identification, the correct assessment may be very crucial. In neurological research, the automatic segmentation of brain MR images plays a vital role [5,8]. In literature, some computer based image segmentation approaches have been developed for the analysis of brain functional arrangements. Among them, thresholding-based, region-based, Markov Random Field and clustering-based methods are the most frequently used segmentation techniques.

Thresholding method [3] uses the intensity histograms and tries to determine intensity values that is called threshold. Threshold partitions the data into target classes and all the pixels are grouped into one class based on thresholds into one class due to which the segmentation is completed. The intensity distribution in medical images, mainly in MRI is mostly complicated and hence, thresholding based methods cannot determine the optimal thresholding value. Tough, computationally, thresholding techniques are well-organized and simple; however, they did not take into account the spatial context of the image and pixel location information is ignored [9]. Region-growing methods [3] extract a connected region consisting of groups of pixels having similar intensities of the image [10]. These methods need starting point commonly known as seed point which is a pixel in the image that fits to the object of attention. The kernel opinion is nominated manually by the user or seed finding algorithm is used which initialize the method automatically. All the adjacent pixels and the associated pixels are added to the growing region due to its examination. Main drawback of region-growing method is the careful initializa-

tion of kernel point and segmentation results might be totally different if the kernel point is selected wrong or different. Another disadvantage of region-growing methods is noise sensitivity. In segmented images, regions are disconnected or there can be holes in the regions in the presence of noise and thus, less preferred for medical image segmentation [3]. Markov Random Field models are basically graphical models and representation of these models is similar to Bayesian Network. Segmentation is performed on the basis of development of models of prior knowledge about the features of image. These image features are edges, labels of regions, contrast and textures etc. The computational cost is very high and requires some extra time to segment an image and that is one of major concerns of this technique [11].

Clustering segmentation approaches [12] are the methods which divide the image into classes of such image pixels which have the similar intensity characteristics without utilizing the training images. Actually these methods utilize available data of image to train themselves. In clustering methods, the training and segmentation happens in parallel. It is an iterative procedure which is performed into two phases: (i) in first step, data is clustered and (ii) in the second step, it estimates the characteristics of each tissue group. The clustering methods are mainly categorized in supervised and unsupervised clustering. Supervised clustering techniques need the clusters number in advance from user, whereas in unsupervised clustering, the cluster information is decided by the clustering system itself. Clustering methods are simple and works better on homogeneous and overlapped regions of the images however, their performance suffers when applied on inhomogeneous regions and also these methods are sensitive to noise. K-means and Fuzzy C-Means are unsupervised clustering techniques used in image processing and medical image segmentation purpose.

K-means is very simple and restrict one image pixel to be only in one group whereas Fuzzy C-Means assign the possibility to each pixel in an image to be in two or more clusters by assigning the membership degrees. The membership degree determines the true position or true class of any pixel [3]. Although the significance of fuzzy c-means method is very satisfactory and successfully applied in real applications, it has some disadvantages as it does not contemplate any spatial context of image and is consequently very subtle to noise and other imaging relic like intensity inhomogeneity. It may also result in local optimum solution caused by poor initialization [9]. In the past, many modifications of fuzzy c-means algorithm have been done in order for making the algorithm further robust to noise and imaging artifacts for image segmentation.

Pham et al. [13] introduced the modified version of FCM as robust FCM (RFCM) by integrating spatial penalty term in the objective function. However, the new objective function suffers from complicated variations in the membership function [14]. A brain MRI segmentation approach has been proposed by Chuang et al. [15] that is named as spatial FCM (sFCM), which adjust the membership function of standard FCM method by incorporating the spatial information. This approach is less subtle to noise and in some extent, this method provides better performance. However, this method still has a problem when the outliers of the image is ruined with seriously noise then this method does not show better performance. Furthermore, this method contains those points in the clusters that are not closer to center of the clusters. Cai et al. [16] developed an approach for brain MR images segmentation using spatial information named as fast generalized Fuzzy C-Means (FGFCM). By using original image along with spatial coordinates and the values of gray level of local neighborhood window, a nonlinearly-weighted sub image is produced. By utilizing nonlinearly-weighted sub image, grouping is applied on the histogram of gray levels for the sub images. The method performs fast; however, still has a problem when the image is ruined with

seriously noise then its performance degrade. Furthermore, directly this algorithm might not be employed on the original image because for noise and robustness, it required suspicious factors collection in order to preserve the features that makes the method complicated [17]. Yu et al. [18] developed a segmentation technique for MRI image. In this approach, fuzzy partition entropy is maximized with 2D histogram. Though the technique produces some improved segmentation results but major drawback of this method is its large time complexity and spends long time in finding the optimal parameters. The authors of [19] proposed a modified version of standard FCM algorithm by modifying the membership function to segment the MRI images. The significance of the method suffers as the level of noise enlarges and reproduces blur images. Caldaïrou et al. [20] proposed an MRI segmentation non-local FCM (NL/FCM) method by updating the main function of the FCM technique. In order to make the algorithm more robust against noise and intensity inhomogeneity, non-local regularization term is integrated with non-local data term and incorporated in the objective function. Zhao et al. [21] developed a modified version of regular FCM for segmentation by adding non-local spatial information in FCM. The performance of this method is better and suppresses more noise effects and deal with inhomogeneity but the performance declines at high noise effects. Ji et al. [22] proposed a brain MRI image segmentation approach by using spatial information which integrates the weighted patch of image with the standard FCM algorithm. The weights have been calculated based on eight neighbors around the central pixel in the squared window. The weights incorporated in the FCM algorithm have been calculated by patch instead of individual pixels in the patch. Though the method effectively reduces MRI noise interference, however, it becomes very complicated, and fails to segment brain tissues accurately [23]. Wang et al. [19] developed a technique for brain MRI segmentation. They modified the main function of regular FCM approached in the presence of noise, by integrating the information-theoretic structure into the normal FCM in order to make the method more robust. The proposed method is much better than of the regular FCM with capability of catering noise problem. However, in the presence of high level of noise, the significance of this method gradually decreased. Alipour et al. [24] developed a segmentation method by merging spatially inhibited kernel-based Fuzzy C-Means method (SKFCM) and a Fast-Two-Cycle (FTC) method. SKFCM creates a rough segmentation to choose the primary contour spontaneously and the partition matrix formed by this algorithm is presented to FTC for segmentation. There is no mechanism to suppress the noise effect. Ali et al. [25] proposed a segmentation method Wavelet Morphological Fusion Fuzzy C-Means (WMMFCM) for brain MRI image. In this approach, first wavelet transform is applied on input image till 3rd levels and obtained the wavelet coefficients at each level. Later these coefficients are fused with original image through using the morphological pyramids to increase the sharpness and decrease the effect of noise. After this the FCM algorithm is employed to the fused images for segmentation. The performance of the technique is better than some previous methods but the resulting images still contains noise. Adhikari et al. [9] proposed the modified version of FCM in order to generate the conditional spatial FCM (csFCM). In this method, membership function of standard FCM is modified to incorporate conditional factors describing the pixel involvement level in order to built clusters and spatial information as well. Regardless of providing better performance, in some cases, this approach misplaces valuable information about tissues. Moreover, the authors also described the limitations that the significance of the their proposed approach decreased in the presence of high level of noise; while the intensity inhomogeneity enlarged. Deng et al. [26] developed the updated version of standard FCM approach by modifying the objective function. In this

method, a new gray-difference coefficient is employed to calculate the consequence of neighboring pixels for enhancing the performance against noise.

Most of the methods that have been reviewed above suffer severely from noise and other noise multiplicative parameter intensity inhomogeneity in the MRI. The intensity inhomogeneity which is also known as intensity non-uniformity (INU) is the non-uniformities of intensities over the same class of tissues or structures. This imaging artifact significantly decreases the performance of any type of image processing algorithm that uses intensities as a feature and also reproduces poor segmentation.

In order to face above challenges and issues, this paper describes a clustering based method weighted spatial fuzzy c-means (wsFCM) by utilizing spatial context of images.

We have already described certain literature review about this field. The rest of the paper is prepared as follows: Section 2 presents an overview of standard FCM algorithm. Section 3 describes the detail of proposed methodology. In Section 4, the evaluation and validation strategy of the proposed method have been represented. The results and discussions have been described in Section 5. The paper will finally be concluded after some discussions in Section 6.

2. Standard Fuzzy C-Means (FCM) method

The standard FCM was developed by [9–14] that was modified by [27] in 1981. The FCM algorithm is a clustering technique where every data point fits to in excess of one cluster. The algorithm starts with an initial guess of randomly picked centers of every cluster. The FCM algorithm attempts to associate each of the data point to one of the clusters by assigning a degree of membership based on likelihood. In clusters, a probability distribution function is utilized to assign the membership degree for each data point. FCM is an iterative method which aims at minimization of an objective function. When each data point becomes closer to their respective clusters centers, the objective function is minimized and algorithm terminates. A higher degree value is allotted to those items which have short distance from cluster center and lower to those which have large distance from that of cluster center. The clusters centers are revised after each of iteration. The objective function of FCM algorithm is given as:

$$J_{FCM} = \sum_{i=1}^N \sum_{j=1}^C U_{ij}^m x_i - v_j^2 \quad (1)$$

where N represents the total items of the data, C indicates the clusters number, v_j represents the center of the cluster j . $\|\cdot\|$ is a norm metric which measures the intimacy of data item x_i to center of the cluster j^{th} , $m(> 1)$ is the fuzziness co-efficient which calculates the acceptance of the compulsory grouping and finds how much the clusters overlays thru one another, and U is the membership matrix which contains the membership degrees. Suppose, we have a data point x_i , then the cluster membership degree j is measured as below:

$$U_{ij} = \frac{1}{\sum_{k=1}^C \left(\frac{x_i - v_j}{x_i - v_k} \right)^{\frac{2}{m-1}}} \quad (2)$$

and the cluster center v_j is calculated as follows:

$$v_j = \frac{\sum_{i=1}^N U_{ij}^m x_i}{\sum_{i=1}^N U_{ij}^m} \quad (3)$$

It is worth to note that as the FCM algorithm starts, the membership degree m for data point i against cluster j is initialized with a casual number between 0 and 1, as below:

$$\sum_j^c U_{ij} = 1$$

3. Proposed methodology

The overall framework of the proposed methodology is represented in Fig. 1. The detail of the proposed methodology is given below in subsections.

3.1. Preprocessing

There are some factors such as noise and the overlapping of tissues intensities make the segmentation a challenging task in brain MR images.

The MR images may possess the noise, which affects the performance and quality of segmentation and also affects the diagnosis of diseases. Therefore, a preprocessing step is important for brain MR images before performing the segmentation. So, for noise removing, recently published method that was based on hybrid genetic filter has been utilized [28].

On the other hand, the isolation of brain and non-brain tissues is considered as an important step for the accurate segmentation. Because, the intensities of brain tissues to illustrate gray matter (GM), white Matter (WM), and cerebrospinal fluid (CSF) may overlap with non-brain tissues like muscles, fats, and bones that may complicate the segmentation process. Therefore, after removing the noise effects, the paper proposed the usage of Brain Extraction Tool [29] for the separation of brain parts and non-brain parts.

3.2. Weighted Spatial Fuzzy C-Means (wsFCM)

The fascinating characteristic of the image is to exceedingly correlate the neighboring pixels with each other. However, this important context does not utilize in the regular FCM approach because it lack of robustness against noise and intensity inhomogeneity.

In order to face and handle these issues, a clustering based method weighted spatial fuzzy c-means (wsFCM) by considering the spatial context of images has been developed for the segmentation of brain MRI images. A spatial function is proposed and incorporated in the membership function of regular fuzzy c-means algorithm. The spatial function fully utilizes the spatial characteristics of the image and assigns weights to the neighboring pixels according to their correlation with central pixel in the neighborhood window. More weights are assigned to those pixels which have low intensity distance and high weights to those which have larger distance from the central pixel in the local neighborhood window. The incorporation of spatial function into membership function expands the heftiness of the approach to noise and intensity inhomogeneity thus providing excellent outcomes of segmentation. The spatial function strengthens the membership function which is helpful in preserving the edges of the regions in the image.

In the proposed method, the segmentation process as clustering problem has been formulated. As clustering is an optimization problem, which is usually described by some objective function and constraint. In the developed approach, the following objective function has been proposed:

$$J_{obj} = \sum_{i=1}^n \sum_{j=1}^c (\mu_{ij})^m x_i - c_j^2, 1 < m < \infty \quad (4)$$

With constraints $\sum_{k=1}^c \mu_k(i, j) = 1$ and $c \neq \phi$.

where x_i is data point, c_j is cluster center in j_{th} cluster, m is fuzziness coefficient that controls the overlapping of clusters with one another, and μ_{ij} , is the modified membership function, which is given as below:

$$\mu_{ij} = \frac{\mu_{ij}^p s_{ij}^q}{\sum_{k=1}^c \mu_{kj}^p s_{kj}^q} \quad (5)$$

where p and q are two factors that control the comparative rank of all functions, and s_{ij} represents the three-dimensional function that is coupled with the membership function. The three-dimensional function s_{ij} is given as:

$$s_{ij} = \sum_{k \in NBH(x_i)} \mu_{jk} \quad (6)$$

Where NBH indicates a squared neighborhood window in three-dimensional domain with center pixel x_i . The three-dimensional context of the image is employed for the development of this three-dimensional function. In this context, the neighboring pixels possess maximum similarity with the center pixel. Due to this correlation, it might be possible that all the neighboring pixels be in the same cluster. In order to utilize the above spatial context, a 5×5 squared window around a pixel with all its possible directions has been used as shown in Fig. 2 Let I_k , ($k = 1, 2, 3, 4$) act for the set of directs allied with the k_{th} center at $(0, 0)$ in spatial neighborhood. These coordinates are shown in Fig. 2, which is given below:

$$I_1 = \{(0, -2), (0, -1), (0, 0), (0, +1), (0, +2)\}$$

$$I_2 = \{(-2, 0), (-1, 0), (0, 0), (+1, 0), (+2, 0)\}$$

$$I_3 = \{(-2, -2), (-1, -1), (0, 0), (+1, +1), (+2, +2)\}$$

$$I_4 = \{(-2, +2), (-1, +1), (0, 0), (+1, -1), (+2, -2)\}$$

$$I_k^{(0)} = I_k \setminus (0, 0) \forall k \text{ from } 1 \text{ to } 4 \text{ (shown in Fig. 2)}$$

In 5×5 window with center (i, j) , we defined $d_{(i,j)}^k$ as the summation of the whole changes between $y_{(i,j+s,j+t)}$ and $y_{(i,j)}$ with

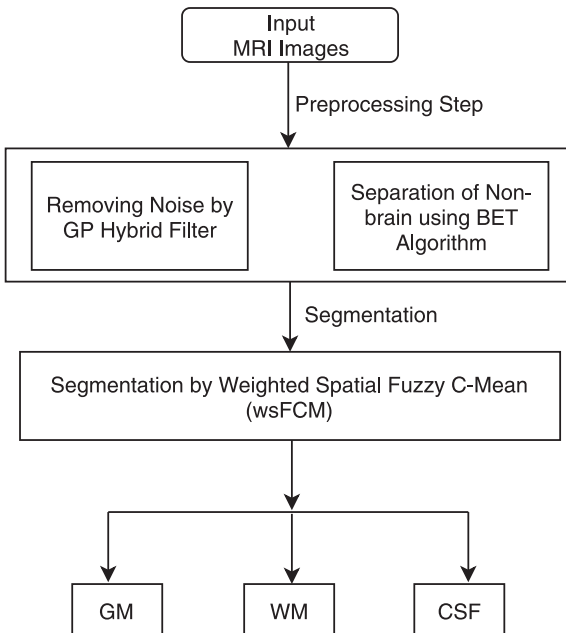


Fig. 1. Architectural diagram for the Proposed Methodology.

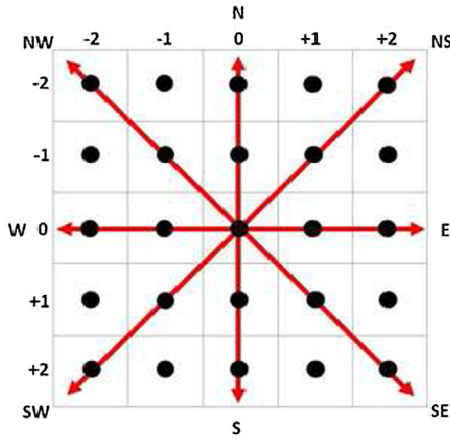


Fig. 2. 5×5 squared neighborhood window.

$(s, t) \in I_k^{(0)}$. If the distance amongst the two pixels in the three-dimension is minor, then their gray values must be closer. Therefore, there might be a chance that both pixels will be the part of the same cluster. We assigned larger weights to those pixels which have least spatial distance along with each direction i.e., $w = 2$ and small weights to remaining directional pixels which have large spatial distances i.e., $w = 1$ before calculating sum. The sum of spatial distances is calculated as:

$$d_{ij}^k = \sum_{s,t \in I_k^{(0)}} w_{s,t} |y_{i+s,j+t} - y_{ij}|, 1 \leq k \leq 4 \text{ and } (s, t) \in \Omega^3 \quad (7)$$

$$\Omega^3 = \{(s, t) : -2 \leq s, t \leq +2\}$$

d_{ij}^k is useful for preserving the edges pixels. This paper calculated the minimum average spatial value along with each direction as given below:

$$d_{min} = \min \{d_{ij}^k \text{ where } 1 \leq k \leq 4\} \quad (8)$$

where d_{min} is the minimum average spatial value among all directions like vertical, horizontal and diagonals. In order to differentiate edges, noisy or irregular and smooth pixels, this paper proposed the usage of a method proposed by Dong [30] with minor changes. The referred method calculated the threshold value by first fixing it and then varying during iterations. The proposed method calculated the threshold value T_w by taking the average of absolute differences along each direction and then compared it with the minimum average value d_{min} . So, for that the following cases has been considered:

Case 1: $d_{min} < T_w$.

This means that the current pixel is a normal pixel, d_{min} is small, because of the four small directional indices.

Case 2: $d_{min} < T_w$.

This implies that, when the present pixel is an edge pixel, d_{min} will be small, because at least one of the direction indices is small.

Case 3: $d_{min} > T_w$.

This implies that, when the present pixel is an irregular pixel, d_{min} will be large, because of the four large directional indices.

In this way, this paper differentiates the smooth, edges and irregular pixels. The edges and smooth pixels are left untreated, preserved and only irregular pixels have been corrected. In order to remove irregularity of the irregular image pixels, the central pixel is replaced with the average intensity values of those pixels which have minimum spatial distance in each direction.

The three-dimension function is integrated in the association function. Similar like association function, the three-dimension

function s_{ij} stands for the possibility that a pixel x_i fits to i^{th} cluster. The three-dimension function of a pixel for a cluster is in height if majority of the neighbors fits to the similar cluster. In a same area, the three-dimension function strengthens the association function and clustering outcome ruins unaffected. But, for noisy or irregular pixels, this function decreases the weighting of noisy or irregular pixels by labeling its neighbors. Consequently, the irregular or misclassified pixels from noisy zones can be classified correctly.

In order to calculate the clusters centers based on modified membership function, this paper used the following function:

$$c_j = \frac{\sum_{i=1}^n \mu_{ij}^m x_i}{\sum_{i=1}^n \mu_{ij}^m} \quad (9)$$

The weighted spatial fuzzy c-means (wsFCM) is described in the Fig. 3. It is obvious from Fig. 3, that the association values are randomly primed; so, that the restraint on the summation of association for every point must be fulfilled. In distinction, additional principles for initialization also occur. For example, the association of a point in the entire classes might be reset along with equal values. But during execution, it followed the accidental initialization principles to create the method reliable along with the regular FCM.

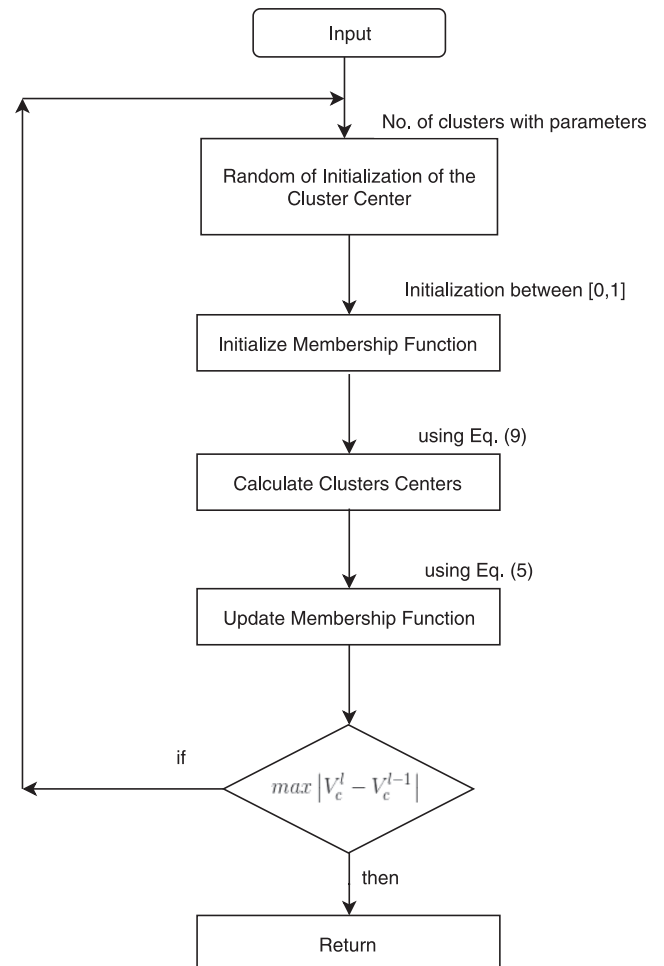


Fig. 3. Descriptive form of the proposed weighted spatial fuzzy c-means (wsFCM) algorithm.

4. Validation of proposed methodology

4.1. Used datasets

We performed a set of experiments on publicly available standard datasets such as simulated and real datasets in order to assess the significance of the proposed segmentation methodology. Each dataset is described as below in subsections.

4.1.1. Simulated dataset

This dataset contains 181 typical images of brain MRI. The normal volume size for such images are $181 \times 217 \times 181$ pixels axial sight learnt at strength non-uniformity ("RF") 20% and 40%, fluctuating different level of noise as 1%–18%, reduction period (TR) 18 ms, reverberation period (TE) 10 ms and piece thickness 1 mm. The modalities employed in order to create such replicated database of MR images are T1-weighted and T2-weighted. Functional replicas for the ground truth are presented in this dataset that is also utilized for the purpose of quantitative evaluation and validation. In this dataset, most of the images have a special file format named NetCDF (MINC), which is commonly used in medical domain, and window cannot read them directly. Therefore, an image-editing tool such as Medical Image Processing Analysis and Visualization (MIPAV) version 7.3.0 [31] was used in order to convert NetCDF (MINC) images to JPEG.

4.1.2. Real dataset

This dataset has been downloaded from Internet Brain Segmentation Repository (IBSR) and its manual was delivered by the Center for Morphometric Analysis at Massachusetts General Hospital [32]. This images in this dataset are "IBSR-V2.0-nifti-st ripped" which were taken from a 35 years old female. This dataset contains of 256 axial sight T1-weighted positionally stabilized revolution, which have a common dimensions 256×128 with piece thickness of 1.5 mm. Manually the anatomical models such as ground truths are utilized for the results validation of the proposed approach.

4.2. Performance parameters

In order to assess the quantitative performance of the proposed method, Dice Similarity Coefficient (DSC), Segmentation Accuracy (SA) and Structured Similarity Index Metric (SSIM) metrics has been used. The DSC, SA and SSIM values closer to 1 indicate better performance of the segmentation methods. Detail of each metric is given below.

4.2.1. Dice Similarity Coefficient (DSC)

Dice Coefficient [33] measures the spatial overlap of two sets. In the segmentation frameworks, this method is used to assess the performance of the segmentation method. In this method, the one set is the segmented image from the method and the other set is the manual segmentation of the same image by the expert. The Dice Similarity Coefficient (DSC) is defined as:

$$DSC_{(A,R)} = \frac{2|A \cap R|}{|A| + |R|} \quad (10)$$

where A indicates the pixels of segmented image extracted by the system and R is the area of brain part image marked by the expert.

4.2.2. Segmentation Accuracy (SA)

The segmentation accuracy (SA) [9] is the ratio of summations of perfectly categorized pixels and total pixels of the clustered image. The SA is defined as follows:

$$SA = \frac{\sum_{i=1}^P \text{cardinality}(A_i \cap C_i)}{\sum_{i=1}^P \text{cardinality}(C_i)} \quad (11)$$

where, A_i , C_i represent the set of pixels in i^{th} cluster formed by the algorithm and reference image respectively, and P denotes the total pixels in a cluster.

4.2.3. Structured Similarity Index Measure (SSIM)

Structured Similarity Index Measure (SSIM) [34] assess the similar details between reference image and segmented images [35]. SSIM can be calculated using equation:

$$SSIM(x, y) = \frac{(2\mu_x\mu_y + C1)(2\sigma_{xy} + C2)}{(\mu_x^2 + \mu_y^2 + C1)(\sigma_x^2 + \sigma_y^2 + C2)} \quad (12)$$

where μ_x, μ_y denote the mean and standard deviations of the referenced and restored images, while σ_{xy} represents their cross correlation in terms of mean and standard deviations of both images. $C1, C2$ represent constants used to control the instability when denominator approaches near to zero.

4.2.4. Similarity Index (P)

Similarity index (p) [36] is employed to measure the similarity between two segmentation. If A_k and B_k represents the pixels in cluster C_i segmented by the method and reference image, then similarity index can be defined as:

$$p = \frac{1}{c} \sum_{k=1}^c \frac{2|A_k \cap B_k|}{|A_k| + |B_k|} \quad (13)$$

The p is ranged in $[0, 1]$, and the best value is 1, which shows the better performance of the algorithm.

4.2.5. Partition Coefficient (PC)

Partition coefficient [36] is widely used to measure the fuzzy partition. The ideal value for P_c is 1 but the values closer to 1 also indicate the better performance of the method. The P_c is defined as:

$$P_c = \frac{\sum_{i=1}^c \sum_{j=1}^N \mu_{ij}^2}{N} \quad (14)$$

4.2.6. Partition Entropy (PE)

Partition entropy [36] measures the entropy of the fuzzy partition. P_c values are ranged in the interval 0 and 1. The optimal value

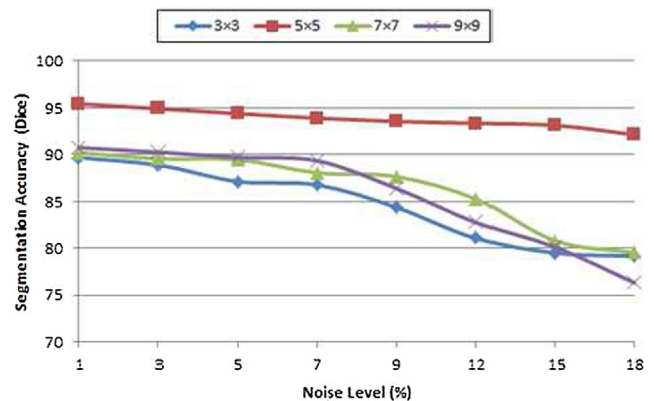


Fig. 4. Effect of different neighborhood window sizes on the performance.

of P_c is 0 but the values nearer to 0 also indicate the better performance.

$$P_c = \frac{\sum_{i=1}^c \sum_{j=1}^N \mu_{ij}^2}{N} \quad (15)$$

4.3. Parameters setting

The parameters p, q of membership function and window size plays a significant role and has effect on the final membership values. The proposed method has been tested with different combination of values of p and q but the significant results achieved when $p = 2$ and $q = 2$ has been used. By considering the spatial context

of the image, a 5×5 square neighborhood window has been used in the proposed method to assign the directional weights to each pixel in the window. Neighborhood plays an important role to select or find out the optimal value in the case of noisy or irregular or for the central pixel. The proposed algorithm is also tested by increasing or decreasing the neighborhood window size, but the algorithm generates better results in case of 5×5 window size. Actually, in the case of 3×3 , all neighboring pixels have same distance from center. In order to cater more neighborhood information especially when the neighborhood of center pixel lies on edges or boundaries of clusters, it is better to consider next neighborhood pixel. Thus in the proposed method 5×5 window has been incorporated. Experimental testing has also been performed to validate it and it works well as comparative to 3×3 . The proposed algorithm has also been tested with 7×7 and 9×9 , but it

Table 1

Accuracy of the proposed segmentation methodology in terms of Dice Similarity Score on simulated T1-weighted dataset images with intensity inhomogeneity (IIH) 20%.

Slice	Tissues	Noise Level								
		0%	1%	3%	5%	7%	9%	12%	15%	18%
#62	GM	0.9634	0.9606	0.9543	0.9503	0.9477	0.9368	0.9313	0.9241	0.9172
	WM	0.9677	0.9654	0.9629	0.9601	0.9584	0.9539	0.9483	0.9427	0.9389
	CSF	0.9468	0.9453	0.9427	0.9398	0.9247	0.9189	0.9132	0.9102	0.9073
#82	GM	0.9659	0.9611	0.9572	0.9507	0.9479	0.9417	0.9401	0.9358	0.9285
	WM	0.9661	0.9649	0.9635	0.9613	0.9589	0.9551	0.9478	0.9456	0.9408
	CSF	0.9388	0.9343	0.9279	0.9243	0.9187	0.9149	0.9114	0.9072	0.9043

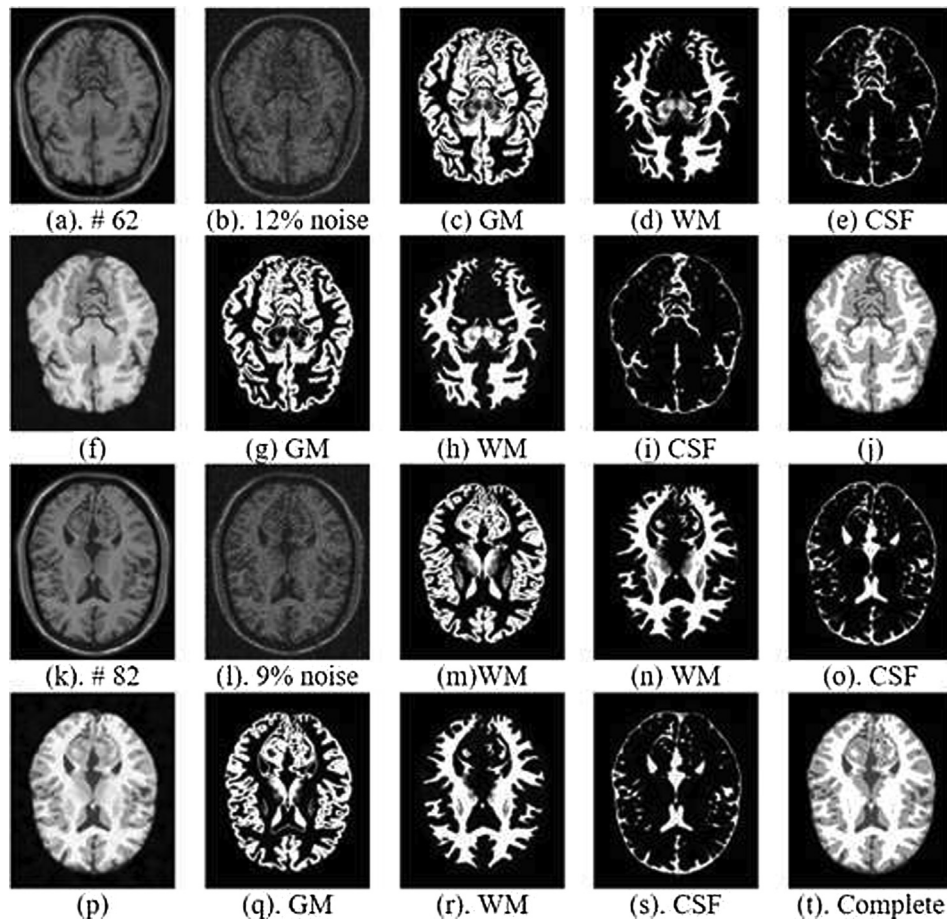


Fig. 5. Qualitative performance of proposed methodology on T1 simulated dataset, (a)–(e) and (k)–(o) are original images, noisy images, GM ground truth, WM ground truth and CSF ground truth respectively, while (f)–(j) and (p)–(t) are noise filtered & skull stripped, segmented GM, segmented WM, segmented CSF and segmented complete images by proposed methodology respectively.

decreases the performance and over-smoothed the edges. Thus in the case of noisy and edge pixels, it is better to use 5×5 window. The segmentation performance of the proposed methodology with different window sizes is shown in Fig. 4.

4.4. Experimental setup

The significance of the developed methodology has been tested and validated on two MRI datasets, for which performed a comprehensive set of experiments under the following setup.

- In the first experiment, the paper has showed the accuracy of the proposed methodology on each dataset individually.
- In the second experiment, the paper has analyzed the robustness of the proposed methodology. For this purpose, a set of four sub-experiments were performed in order for showing the effectiveness of sub-components of the proposed methodology. In the first case, the performance of the proposed framework has been validated without performing preprocessing step and having intensity inhomogeneity. In the second case, the performance has been tested and validated without performing preprocessing step and without intensity inhomogeneity. While, in the third case, the performance has been assessed with performing preprocessing step and without intensity inhomogeneity. Finally, in the last case, the performance of the proposed framework has been analyzed with performing

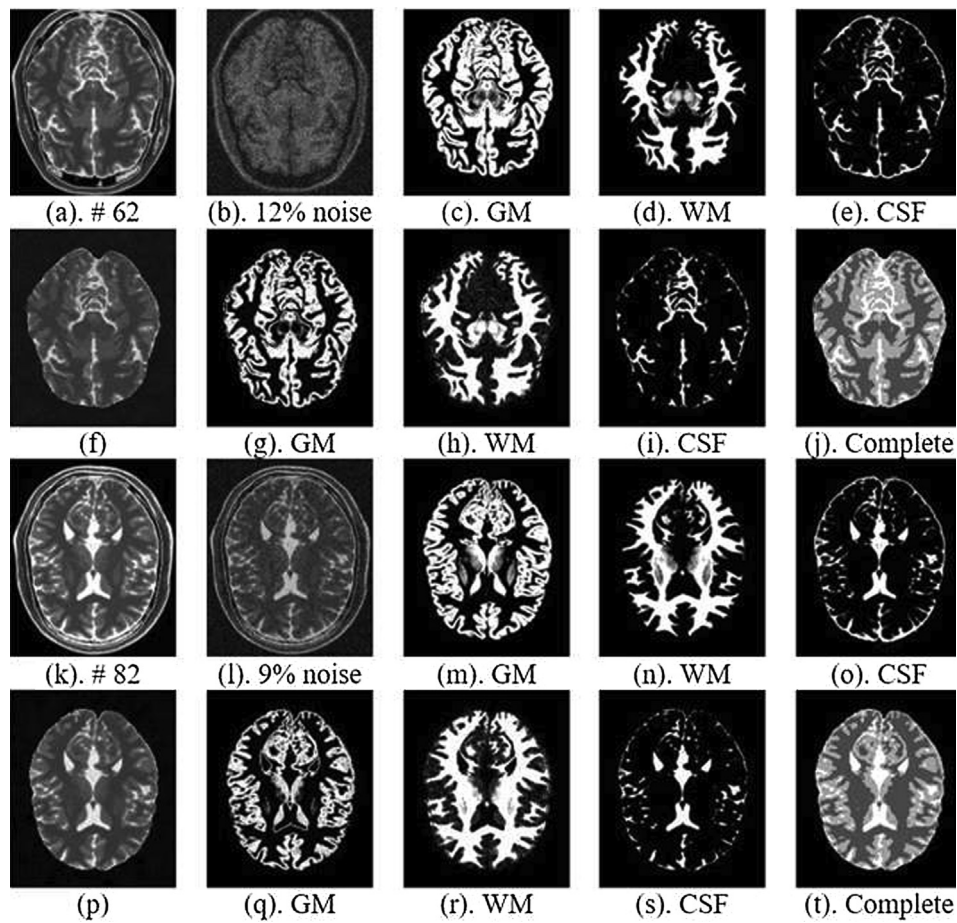


Fig. 6. Qualitative performance of proposed methodology on T2 simulated dataset, (a)–(e) and (k)–(o) are original images, noisy images, GM ground truth, WM ground truth and CSF ground truth respectively, while (f)–(j) and (p)–(t) are noise filtered & skull stripped, segmented GM, segmented WM, segmented CSF and segmented complete images by proposed methodology respectively.

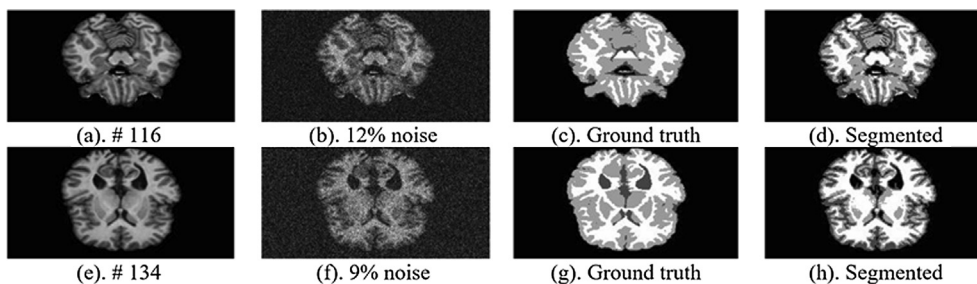


Fig. 7. Qualitative performance of proposed methodology on T1 real dataset, (a) and (e) are original images, (b) and (f) are noisy images, (c) and (g) are ground truth images, while (d) and (h) segmented images by proposed methodology.

preprocessing step and having intensity inhomogeneity in the images.

- Lastly, in this experiment, the paper has performed a series of experiments for comparison in order to show the efficacy of the developed methodology. In this experiment, the significance of the developed methodology was compared against recent methods. The researcher borrowed the implementations for some of the methods, whereas for other methods, he has implemented his respective methods for fair comparison.

5. Results and discussion

In this section, the experimental results of the developed segmentation methodology named weighted spatial Fuzzy C-Means (wsFCM) are presented. The proposed segmentation method is tested both on simulated and real datasets to evaluate and validate the performance of the method. The results are shown in Table 1 and Figs. 5–10 respectively. Figs. 5–7 show the qualitative performance of the proposed segmentation methodology on simulated T1, simulated T2 and real T1 datasets images respectively at different noise levels. In order to get the accurate segmentation results, first the input image is processed for noise suppression and isolation of brain part from non-brain tissues to avoid the overlapping issue which can effect on the segmentation performance and causes to misclassification of the image objects. After performing processing step, the segmentation is performed by the proposed method wsFCM. Also, from the Figs. 5–7, it is obvious that the developed technique succeeded well in correcting and classifying the tissues classes of the images and the brain segmented classes have maximal similarity with reference images.

Edges plays significant role in making the image regions distinct and tracing the symptoms of diseases. Table 2 and Figs. 8–10 show the performance of the proposed segmentation methodology in preserving the edges and structural information on T1 simulated, T2 simulated and T1 real datasets with zooming views. Also, from Figs. 8–10, it is clear that the edges of the segmented images by the developed method have maximum similarity with the structure and edges of reference images (ground truth). This maximum similarity of edges of segmented images between proposed methodology and reference images clearly point towards the better preservation of the edges and structural information. It can be concluded by qualitative inspections of the images, the

proposed algorithm produces a segmentation that accepts maximal similarity with the ground truth and better preservation of the image features such as edges.

Tables 3–6 show the quantitative performance of the proposed segmentation method in preserving edges and structural detail in terms of structured similarity scores on simulated T1, simulated T2 and real T1 datasets images respectively at different noise levels ranging from 0% to 18%. First the edges of the reference and segmented (proposed method) images have been detected using Sobel filter (Sobel & Feldman, 1968) and compared the similarity of edges between reference and segmented images using SSIM. From Tables 1,2, it is obvious that the developed method preserves the sufficient edges information and retains the maximum structure of image at low and high noise levels which indicate the better significance of the proposed segmentation methodology in preserving edges.

From the qualitative and quantitative inspections/ results, it is observed that the developed segmentation method performs sufficient in segmenting the images, preserving edges and generates good results, sustains its performance at increasing levels of noise

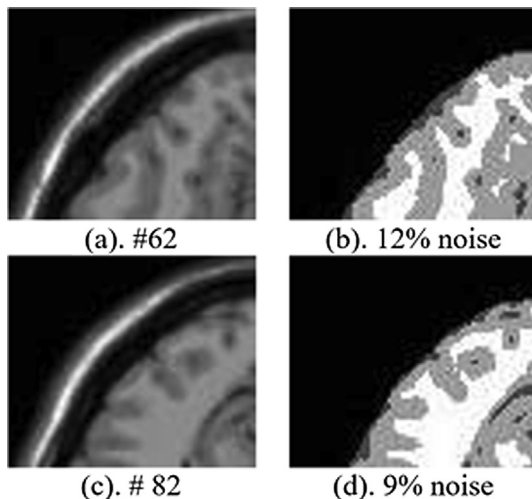


Fig. 8. Qualitative performance of proposed methodology in preserving edges on T1 simulated dataset having 20% intensity inhomogeneity with zooming view, (a) and (c) are original images, (b) and (d) are segmented by proposed method by filtering 12% and 9% noise.

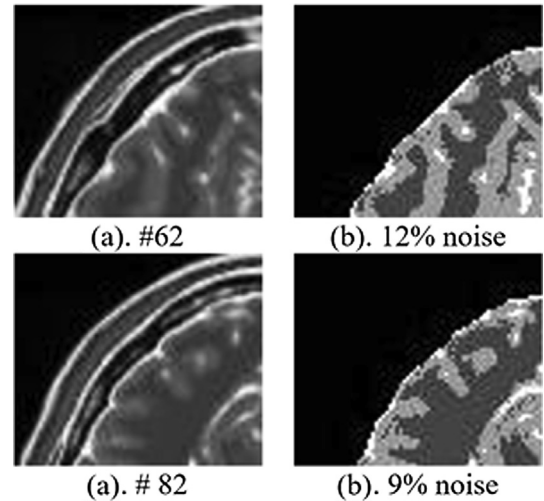


Fig. 9. Qualitative performance of proposed methodology in preserving edges on T2 simulated dataset having 20% intensity inhomogeneity with zooming view, (a) and (c) are original images, (b) and (d) are segmented by proposed method by filtering 12% and 9% noise.

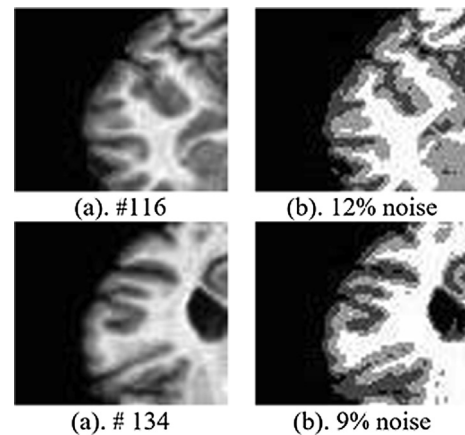


Fig. 10. Qualitative performance of proposed methodology in preserving edges on T1 real dataset image with zooming view, (a) and (c) are original images, while (b) and (d) are segmented by proposed method by filtering 12% and 9% noise.

and suitable for the segmentation of brain MRI. This is all achieved by preprocessing the image properly for handling noise and tissues overlapping issues. The proposed segmentation method also has the capability of handling intensity inhomogeneity, which occurs during image acquisition process by utilizing the spatial characteristics of the image. Therefore, it is obvious that the developed segmentation technique showed a significant performance on standard datasets. It is because, the proposed method first pre-processed the image. Then the three-dimensional context of the image is considered, utilized and integrated in the proposed segmentation method. On the basis of spatial context, weights are assigned to each neighboring pixel in each possible directions of a central pixel in the neighborhood which contribute to decrease the effect of noise itself as well as handling the intensity inhomogeneities occurred during image acquisition process and based on

the directional weights, preserves the edges information. That is why the efficacy of the developed segmentation method is superior.

5.1. Robustness of proposed methodology

As mentioned before, in this experiment, four sub experiments has performed to show the robustness of the proposed methodology to dynamic environments. The detail of each experiment is given below.

Case1: Without Preprocessing and with IIH:

In this experiment, the preprocessing step for noise removal and handling tissues intensities overlapping is not performed. The overall results for this experiment are shown in Fig. 11 and in Table 7.

Table 2

Accuracy of the proposed segmentation methodology in terms of Dice Similarity Score on simulated T2-weighted dataset images with intensity inhomogeneity (IIH) 20%.

Slice	Tissues	Noise Level								
		0%	1%	3%	5%	7%	9%	12%	15%	18%
#62	GM	0.9687	0.9639	0.9602	0.9588	0.9522	0.9450	0.9384	0.9315	0.9261
	WM	0.9701	0.9684	0.9627	0.9604	0.9579	0.9547	0.9500	0.9453	0.9376
	CSF	0.9532	0.9471	0.9406	0.9387	0.9321	0.9257	0.9207	0.9156	0.9111
#82	GM	0.9677	0.9640	0.9614	0.9573	0.9524	0.9479	0.9407	0.9368	0.9386
	WM	0.9713	0.9681	0.9645	0.9618	0.9587	0.9534	0.9487	0.9451	0.9413
	CSF	0.9549	0.9522	0.9389	0.9357	0.9316	0.9284	0.9224	0.9184	0.9072

Table 3

Accuracy of the Proposed Segmentation methodology in terms of Dice Similarity Score on real T1-weighted dataset images.

Slice	Tissues	Noise Level								
		0%	1%	3%	5%	7%	9%	12%	15%	18%
#116	GM	0.9707	0.9682	0.9642	0.9614	0.9566	0.9531	0.9497	0.9423	0.9367
	WM	0.9759	0.9713	0.9671	0.9623	0.9568	0.9577	0.9462	0.9426	0.9385
	CSF	0.9486	0.9445	0.9413	0.9393	0.9354	0.9308	0.9288	0.9211	0.9162
#134	GM	0.9717	0.9671	0.9642	0.9582	0.9546	0.9523	0.9382	0.9218	0.9116
	WM	0.9804	0.9766	0.9719	0.9673	0.9633	0.9615	0.9584	0.9525	0.9463
	CSF	0.9523	0.9489	0.9471	0.9433	0.9386	0.9353	0.9310	0.9254	0.9186

Table 4

SSIM based significance of the developed segmentation methodology in preserving edges on simulated T1-weighted images.

Slice	Noise Level								
	0%	1%	3%	5%	7%	9%	12%	15%	18%
#62	0.9713	0.9691	0.9532	0.9471	0.9384	0.9246	0.9169	0.9019	0.8938
#82	0.9761	0.9627	0.9569	0.9491	0.9381	0.9303	0.9241	0.9109	0.8856

Table 5

SSIM based significance of the developed segmentation methodology in preserving edges on simulated T2-weighted images.

Slice	Noise Level								
	0%	1%	3%	5%	7%	9%	12%	15%	18%
#62	0.9685	0.9625	0.9543	0.9432	0.9311	0.9261	0.9137	0.9016	0.8915
#82	0.9693	0.9619	0.9557	0.9449	0.9298	0.9221	0.9187	0.9033	0.8942

Table 6

SSIM based significance of the developed segmentation methodology in preserving edges on real T1-weighted images.

Slice	Noise Level								
	0%	1%	3%	5%	7%	9%	12%	15%	18%
#116	0.9769	0.9724	0.9681	0.9573	0.9518	0.9354	0.9204	0.9133	0.9010
#134	0.9748	0.9717	0.9669	0.9491	0.9407	0.9383	0.9241	0.9109	0.8986

It is clear from Fig. 11 and in Table 7 that the preprocessing step for handling noise and tissues overlapping issues has an important role in achieving best accuracy for the proposed method. This is because the noise in images has direct influence on the quality and accuracy of the segmentation. Moreover, Fig. 11 also presents

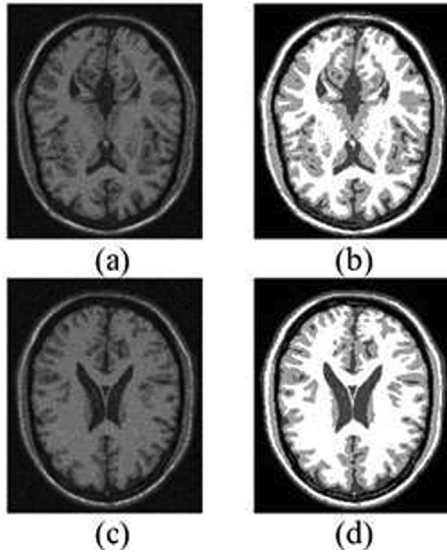


Fig. 11. Qualitative results of the proposed methodology without image preprocessing and with intensity inhomogeneity (IIH), (a) and (c) are original images with noise, (b) and (d) segmented images.

Table 7

Dice Similarity based quantitative results of the proposed methodology without preprocessing and with intensity inhomogeneity (IIH) using simulated T1-weighted images dataset.

Environment	Slice	Segmentation Accuracy
Without Preprocessing and IIH = 20%	#77	0.8885
	#93	0.8947
	Average	0.8916

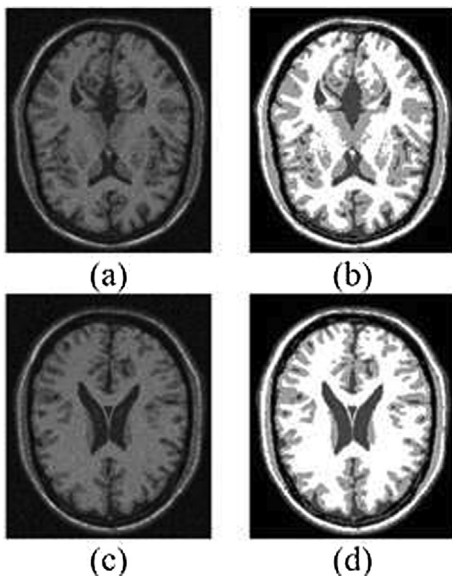


Fig. 12. Qualitative results of the proposed methodology with image preprocessing and without intensity inhomogeneity (IIH), (a) and (c) are original images with noise, (b) and (d) segmented images.

Table 8

Dice Similarity based quantitative results of the proposed methodology without preprocessing and without intensity inhomogeneity (IIH) using simulated T1-weighted images dataset.

Environment	Slice	Segmentation Accuracy
Without Preprocessing and IIH = 0%	#77	0.8902
	#93	0.8940
	Average	0.8921

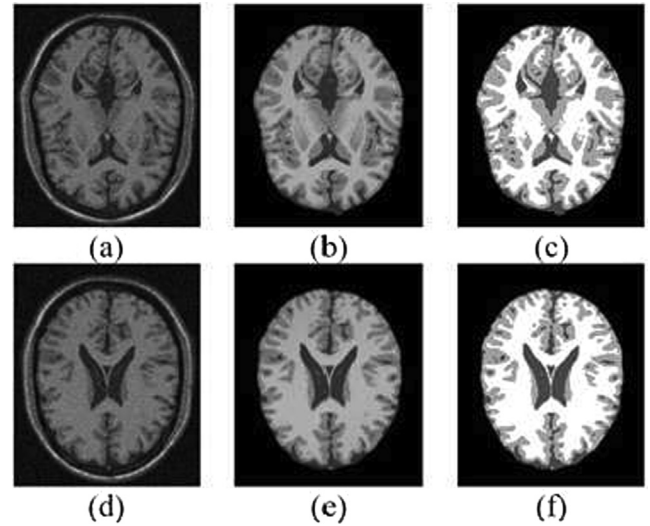


Fig. 13. Qualitative results of the proposed methodology with image preprocessing and with intensity inhomogeneity (IIH), (a) and (d) are original images with noise, (b) and (e) are preprocessed images and, (c) and (f) segmented images.

Table 9

Dice Similarity based quantitative results of the proposed methodology with preprocessing and with intensity inhomogeneity (IIH = 20%) using simulated T1-weighted images dataset.

Environment	Slice	Segmentation Accuracy
With Preprocessing and IIH = 20%	#77	0.9234
	#93	0.9320
	Average	0.9255

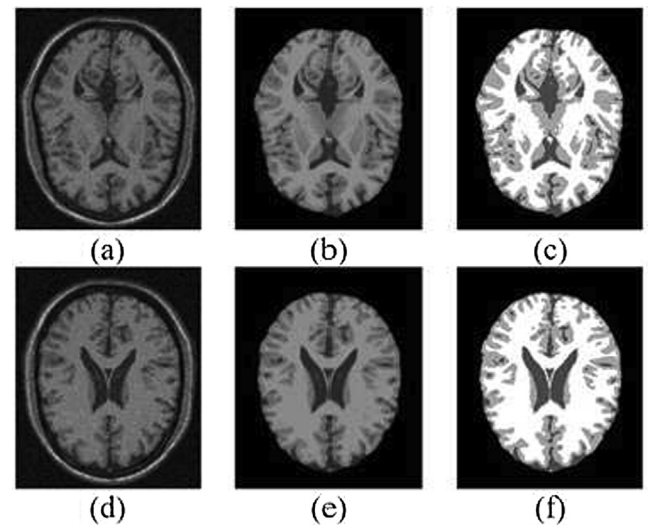


Fig. 14. Qualitative results of the proposed methodology with image preprocessing and with intensity inhomogeneity (IIH), (a) and (c) are original images with noise, (b) and (d) segmented images.

Table 10

Dice Similarity based quantitative results of the proposed methodology with preprocessing and with intensity inhomogeneity (IIH = 0%) using simulated T1-weighted images dataset.

Environment	Slice	Segmentation Accuracy
With Preprocessing and IIH = 0%	#77	0.9209
	#93	0.9301
	Average	0.9277

Table 11

Quantitative comparison of proposed methodology with previous different methods on 51 T1-weighted simulated dataset images in term of cluster validity functions.

Image Volume	Method	Clusters Validation		
		P _c	P _e	p
IIH = 40%, Noise = 9%	FCM	0.803	0.378	71.176
	sFCM	0.897	0.180	74.351
	FGFCM	0.584	0.777	71.217
	ASIFC	0.843	0.290	75.580
	csFCM	0.943	0.096	76.670
	wsFCM	0.955	0.068	78.751
IIH = 20%, Noise = 9%	FCM	0.803	0.378	71.612
	sFCM	0.897	0.180	75.023
	FGFCM	0.600	0.748	71.564
	ASIFC	0.845	0.299	76.428
	csFCM	0.945	0.094	77.594
	wsFCM	0.961	0.062	79.014
IIH = 40%, Noise = 7%	FCM	0.823	0.343	75.656
	sFCM	0.910	0.157	76.943
	FGFCM	0.592	0.762	74.782
	ASIFC	0.844	0.309	76.980
	csFCM	0.947	0.089	77.509
	wsFCM	0.966	0.063	79.339
IIH = 20%, Noise = 7%	FCM	0.823	0.343	75.653
	sFCM	0.912	0.153	77.723
	FGFCM	0.613	0.724	75.380
	ASIFC	0.866	0.294	77.072
	csFCM	0.949	0.086	78.493
	wsFCM	0.969	0.058	80.026

Table 12

Quantitative comparison of proposed methodology with previous different methods on 51 T1-weighted simulated datasets images in term of average segmentation accuracy.

Image Volume	Method	Segmentation Accuracy (SA)		
		CSF	GM	WM
IIH = 40%, Noise = 9%	FCM	0.791	0.786	0.820
	sFCM	0.832	0.863	0.869
	FGFCM	0.777	0.782	0.878
	ASIFC	0.852	0.866	0.891
	csFCM	0.880	0.877	0.921
	wsFCM	0.909	0.917	0.942
IIH = 20%, Noise = 9%	FCM	0.797	0.792	0.824
	sFCM	0.831	0.872	0.890
	FGFCM	0.779	0.783	0.894
	ASIFC	0.856	0.885	0.926
	csFCM	0.884	0.890	0.947
	wsFCM	0.913	0.935	0.957
IIH = 40%, Noise = 7%	FCM	0.843	0.855	0.847
	sFCM	0.888	0.896	0.909
	FGFCM	0.853	0.836	0.912
	ASIFC	0.890	0.899	0.913
	csFCM	0.903	0.902	0.933
	wsFCM	0.917	0.931	0.944
IIH = 20%, Noise = 7%	FCM	0.847	0.858	0.852
	sFCM	0.889	0.905	0.935
	FGFCM	0.856	0.844	0.932
	ASIFC	0.891	0.907	0.939
	csFCM	0.902	0.915	0.959
	wsFCM	0.919	0.942	0.961

that the noise affects the quality of the segmented images and the homogeneous regions still contain the noisy pixels. The noise also exists on the boundaries of the regions due to which the regions boundaries are not clear and overlapping. Also the accuracy of the proposed segmentation method is suffered due to noise as given in Table 7. On the other hand, intensity inhomogeneity issue degrades image quality and causes to reproduce the poor segmentation. However, the developed method has the inbuilt capability of dealing with intensity inhomogeneity and handling other irregularities due to which the method still sustains its accuracy but not achieved much better results due to noise effect. It can be concluded that the preprocessing of image is an important step of the method and has a significant role in achieving the best accuracy of the proposed segmentation method.

Case2: Without Preprocessing and without IIH:

In this experiment, preprocessing step is not performed and presented image to proposed segmentation method which contain no inhomogeneity. The overall results for this experiment are represented in Fig. 12 and Table 8.

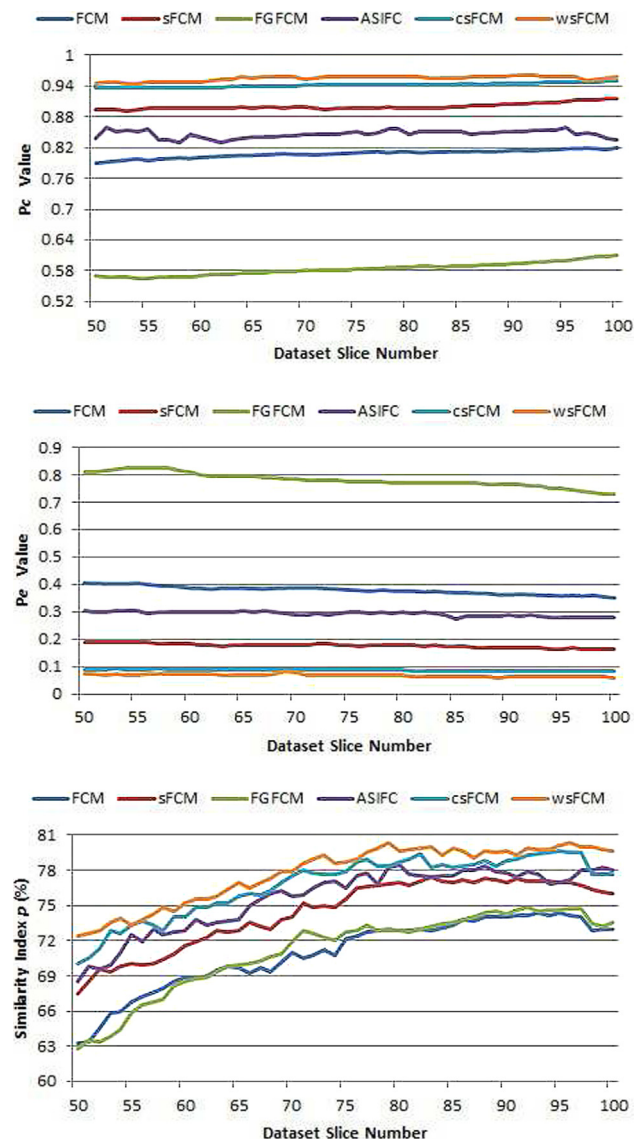


Fig. 15. Quantitative comparison of proposed methodology with previous different methods on 51 T1-weighted simulated dataset images in term of average segmentation accuracy (Top) CSF, (Middle) GM and (Bottom) WM.

From Fig. 12 and Table 8, it can be observed that the preprocessing step has a significant role in achieving the best accuracy for the proposed method. This is because the effect of noise is not first properly reduced from the images due to which the visual quality of the segmentation and overall accuracy of the segmentation method is affected. The performance of the proposed method is satisfactory due to capability of handling imaging irregularities if exist in the images but not much better as the noise is not removed properly. So, it can be concluded that the processing of image is necessary in the segmentation framework, which plays an essential role in achieving the better accuracy and results.

Case3: With Preprocessing and with IHH:

Fig. 13 and Table 9 show the qualitative and quantitative outcomes of the proposed segmentation method with performing preprocessing step and its role in the methodology in achieving the best accuracy. From Fig. 13, it can be perceived from segmented images that the proposed segmentation method reproduces the good segmentation quality with homogeneous regions having sharp and clear regions boundaries. The reason behind this is the proper noise suppression and isolation of brain and non-brain parts and presenting the noise free image to the segmentation method. The preprocessing of image as well as utilization of the spatial characteristics of the images adds value to the proposed segmentation methodology in achieving the best accuracy of the segmentation. Also, from the Fig. 13 and Table 9, it can be concluded that the performance of the proposed segmentation methodology is reliant on resolving noise and tissue intensities overlapping issues properly along with other inbuilt capabilities of intensity inhomogeneity handling in reproducing good segmentation and achieving best accuracy.

From Fig. 13 and Table 9, it can be observed that the preprocessing step has a significant role in achieving the best accuracy for the proposed method. This is because the effect of noise is not first properly reduced from the images due to which the visual quality of the segmentation and overall accuracy of the segmentation method is affected. The performance of the proposed method is satisfactory due to capability of handling imaging irregularities if exist in the images but not much better as the noise is not removed properly. So, it can be concluded that the processing of image is necessary in the segmentation framework, which plays an essential role in achieving the better accuracy and results.

Case4: With Preprocessing and without IHH:

Fig. 14 and Table 10 illustrate the significant function of the preprocessing step in achieving the best qualitative and quantitative results of proposed segmentation methodology. This is because the noise is suppressed properly from the images and isolated the non-brain parts and capability of the proposed method itself in dealing with the intensity inhomogeneity issue by considering and incorporating the spatial context of the image.

As can be observed from Fig. 14, each region in the segmented images is distinct with clear boundaries and free of noise and the overall accuracy of the proposed methodology is much better as given in Table 10. From this sub experiment, it can be concluded that the preprocessing of images is a very important step of the methodology, which strengthens the performance of the segmentation methodology in achieving best accuracy.

Based on the above experimentations and results achieved, it has been proved that the proposed segmentation methodology showed best performance in the presence of imaging artifacts and intensity inhomogeneity as well as in the absence of imaging artifacts and intensity inhomogeneity. It is clear from these experiments that the proposed method sustained its accuracy in noisy and noise free environments, which means that the proposed methodology is more robust to dynamic environments.

5.2. Comparison

The article has discussed and compared the results attained from the developed approach against existing methods showed in Table 11 and Fig. 15. We attained these results using brain images of MRI along with 7%–9% of noise level and 20%–40% intensity inhomogeneity on 51 simulated dataset T1-weighted images (pieces 50–100). Fig. 15 shows a comparison of the proposed methodology with existing methods, that is, sFCM, FGFCM, ASIFC and csFCM in terms of cluster validity functions like partition coefficient (P_c), partition entropy (P_e) and similarity index (p) over 51 T1-weighted simulated dataset images (50–100). Also from Fig. 15, it can be perceived that the developed technique performs well than existing methods and sustains its superiority which clearly points towards the better performance. Fig. 16 shows the quantifiable relative values of segmentation of gray matters (GM), white matters (WM) and cerebrospinal fluid (CSF) tissues of proposed methodology with previous different methods fuzzy c-means (FCM), spatial fuzzy c-means (sFCM), fuzzy generalized

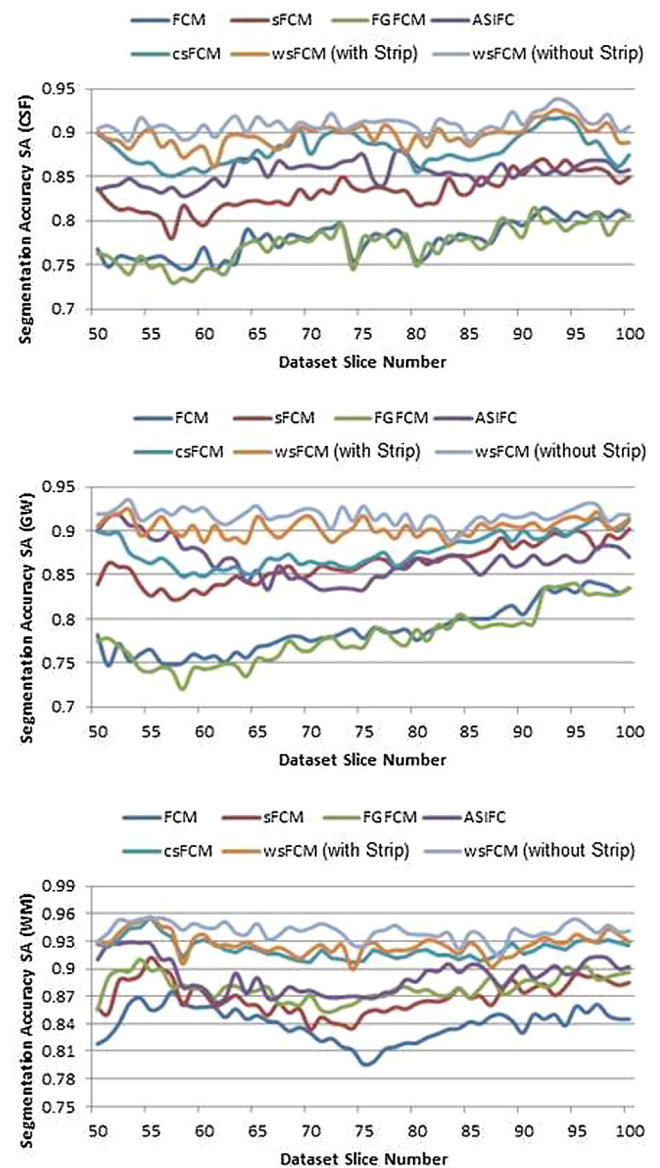


Fig. 16. Quantitative comparison of proposed methodology with previous different methods on 51 T1-weighted simulated dataset images in term of average segmentation accuracy (Top) CSF, (Middle) GM and (Bottom) WM without strip.

fuzzy c-means (FGFCM), adaptive spatial information fuzzy clustering (ASIFC) and conditional spatial fuzzy c-means (csFCM) on 51 T1-weighted simulated dataset images (slices 50–100) with 9% noise and 40% intensity inhomogeneity. It is clear that the developed technique consistently outperforms than the competitors state-of-the-art algorithms while segmenting the tissues regions. It can also be observed that the previous algorithms per-

form better on some images while the proposed method performance is better and consistent on all tested images. The results show that overall performance of proposed method is constantly better although the efficacy degrade if brain and non-brain parts do not correctly separated.).

Table 11 shows a comparison of the developed approach along with previous methods, that is, FCM, sFCM, FGFCM, ASIFC and

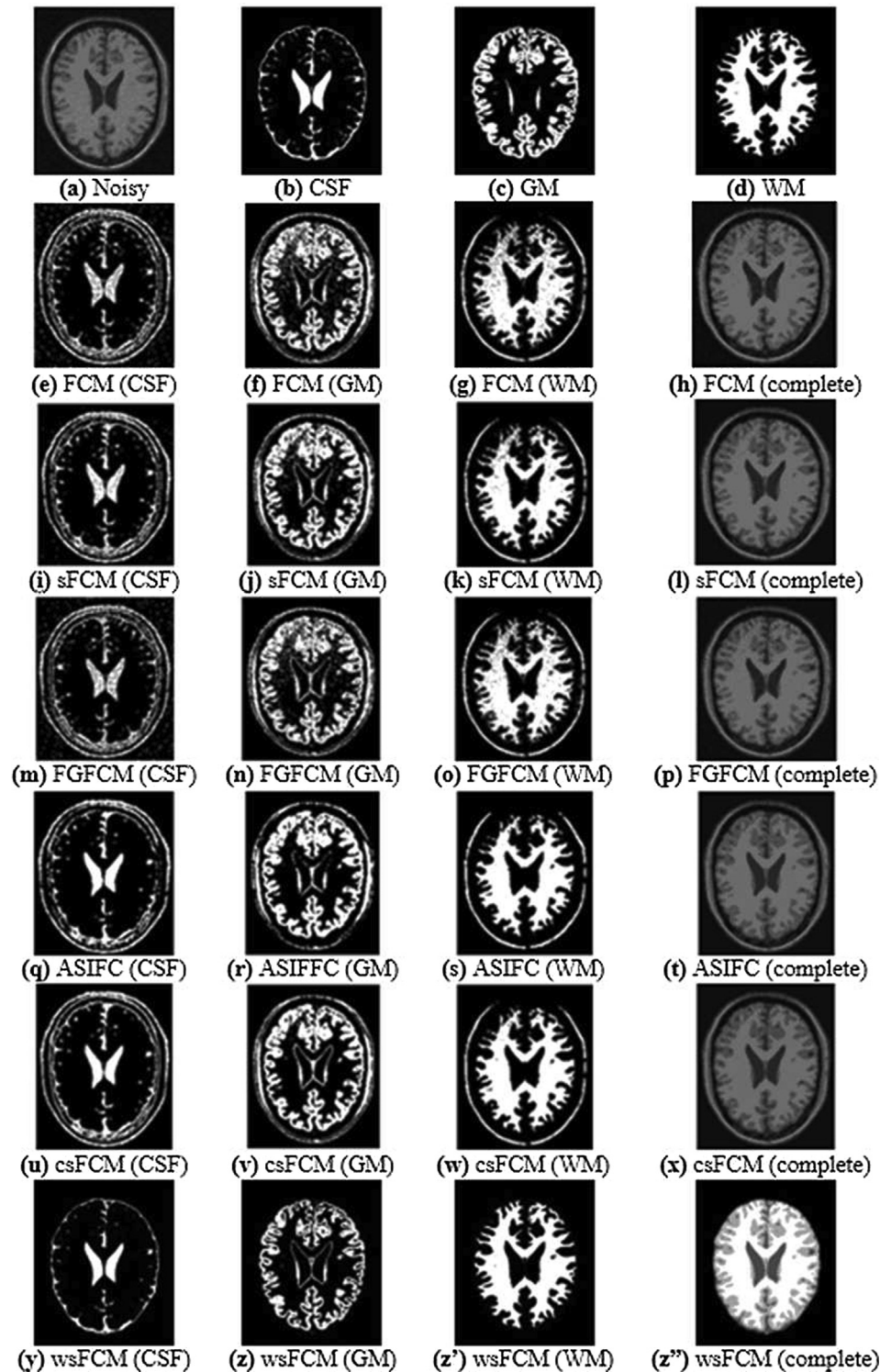


Fig. 17. Sample segmentation results of CSF, GM, WM against state of the art techniques on a T1-weighted images in simulated dataset (piece No. 95) with 9% level of noise and 40% inhomogeneity. (a): Original noisy image; (b)–(d): Ground Truths; (e)–(h): FCM; (i)–(l): sFCM; (m)–(p): FGFCM; (q)–(t): ASIFC; (u)–(x): csFCM; (y)–(z): developed methodology (wsFCM).

csFCM in terms of averaged values of diverse cluster rationality functions such as partition coefficient (Pc), partition entropy (P_e) and similarity index (P) over 51 T1-weighted simulated dataset images (50–100). From Table 11, it can be observed that the average values of Pc and P_e generated by new method are near to 1 and 0 correspondingly under the presence of highest values of noise and inhomogeneity, whereas, the performance of the other competitor methods is not well. In each dataset images, the value of similarity index p of the proposed method is increased than existing methods which shows that the proposed method outperforms.

Table 12 also shows the quantitative comparisons of proposed method with sFCM, FGFCM, ASIFC and csFCM in terms of segmentation accuracy of GM, WM and CSF regions over 51 T1-weighted simulated dataset images (slices 50–100) with 7%–9% level of noise and 20%–40% intensity inhomogeneity. From the results, we can observe that the developed technique produces significant results against recent methods. The segmentation accuracy of the previous algorithms suffers as the intensity inhomogeneity in the images increases.

Fig. 17 presents the qualitative assessment of the developed approach along with previous methodologies on T1-weighted simulated dataset (slice 95) with noise level 9% and intensity inhomogeneity 40%. It is obvious that the existing approaches consistently faced certain problem in which some tissues incorrectly categorized. Hence, these approaches did not focus on eliminating the non-brain portions from brain portions because of that intensities overlying happen, which degrade the accuracy of segmentation. Out of standard methods, csFCM shows significant performance against existing methods. On the other side, the developed methodology has come advantages such as noise removal in pre-processing, separation of brain and non-brain materials, edge conservation, and mechanism to correctly handle intensity inhomogeneity, because of these advantage, the our approach showed significant performance against existing techniques.

6. Conclusions

In this paper, a robust clustering based technique weighted spatial fuzzy c-means (wsFCM) by utilizing spatial context of images has been developed for the segmentation of brain MRI. In the proposed algorithm, a spatial function is proposed and incorporated in the membership function of regular fuzzy c-means technique. The spatial function considers and utilizes the spatial characteristics of the image and assigns weights to the neighbors according to their correlation with central pixel in the neighborhood window. The incorporation of spatial function into membership function improves the robustness of the algorithm to noise and intensity inhomogeneity thus providing excellent outcomes of segmentation. The spatial function strengthens the membership function which is helpful in preserving the edges of the regions in the image. The proposed method is tested on two publicly available standard datasets, BrainWeb simulated and IBSR real. A comprehensive set of experimentation is performed in order to evaluate and validate performance of proposed algorithm through standard metrics. The results showed that the performance of the proposed method is robust to noise and deals with the intensity inhomogeneity issue with a better and improved way. The performance of the developed methodology is compared against recent algorithms and performance found to be superior to existing techniques in this domain.

Acknowledgment

This work was supported by the Jouf University, Sakaka, Aljouf, Kingdom of Saudi Arabia under the registration No. 37/438.

References

- [1] Du Y, Lai P, Leung C, Pong P. Design of superparamagnetic nanoparticles for magnetic particle imaging (MPI). *Int J Mol Sci* 2013;14(9):18682–710.
- [2] Yang J, Fan J, Ai D, Zhou S, Tang S, Wang Y. Brain MR image denoising for Rician noise using pre-smooth non-local means filter. *Biomed Eng Online* 2015;14(1):2.
- [3] Despotovic I, Goossens B, Philips W. MRI segmentation of the human brain: challenges, methods, and applications. *Computational and mathematical methods in medicine*; 2015..
- [4] Long-term study plays down risk of brain problems in HIV-positive patients. <http://www.aidsmap.com/Long-term-study-plays-down-risk-of-brain-problems-in-HIV-positive-patients/page/1423648> [accessed: 2019-03-20].
- [5] Kumar PS, Kumar PG. Performance analysis of brain tumor diagnosis based on soft computing techniques. *Am J Appl Sci* 2014;11(2):329–36.
- [6] Miao Z, Lin X, Liu C. Automatic segmentation of brain tissue based on improved fuzzy c means clustering algorithm. *J Biomed Sci Eng* 2011;4:100–4.
- [7] Lewis T, Writer S. Human brain: Facts, functions & anatomy; 2016. [accessed: 2019-03-20].
- [8] Riad AM, Atwan A, El HM, Mostafa RR, Elminir HK, Mastorakis N. A new approach for segmentation of brain MR image. *Proceedings of the WSEAS International Conference on Environment, Medicine and Health Sciences*, vol. 5125. p. 74–83.
- [9] Adhikari SK, Sing JK, Basu DK, Nasipuri M. Conditional spatial fuzzy c-means clustering algorithm for segmentation of MRI images. *Appl Soft Comput* 2015;34:758–69.
- [10] Haralick RM, Shapiro LG. Image segmentation techniques. *Computer Vision, Graphics, and Image Processing* 1985;29(1):100–32.
- [11] Roy S, Nag S, Maitra IK, Bandyopadhyay SK. A review on automated brain tumor detection and segmentation from MRI of brain. *arXiv preprint arXiv:1312.6150*.
- [12] Liu J, Li M, Wang J, Wu F, Liu T, Pan Y. A survey of MRI-based brain tumor segmentation methods. *Tsinghua Sci Technol* 2014;19(6):578–95.
- [13] Pham DL. Fuzzy clustering with spatial constraints. *Proceedings. International Conference on Image Processing*, vol. 2. IEEE; 2002. pp. II–II.
- [14] Shen S, Sandham W, Granat M, Sterr A. MRI fuzzy segmentation of brain tissue using neighborhood attraction with neural-network optimization. *IEEE Trans Inf Technol Biomed* 2005;9(3):459–67.
- [15] Chuang K-S, Tzeng H-L, Chen S, Wu J, Chen T-J. Fuzzy c-means clustering with spatial information for image segmentation. *Comput Med Imaging Graph* 2006;30(1):9–15.
- [16] Cai W, Chen S, Zhang D. Fast and robust fuzzy c-means clustering algorithms incorporating local information for image segmentation. *Pattern Recognition* 2007;40(3):825–38.
- [17] Jiang X-L, Wang Q, He B, Chen S-J, Li B-L. Robust level set image segmentation algorithm using local correntropy-based fuzzy c-means clustering with spatial constraints. *Neurocomputing* 2016;207:22–35.
- [18] Yu H-Y, Fan J-L. Three-level image segmentation based on maximum fuzzy partition entropy of 2-d histogram and quantum genetic algorithm. In: *International Conference on Intelligent Computing*. Springer; 2008. p. 484–93.
- [19] Wang Z, Song Q, Soh YC, Sim K. An adaptive spatial information-theoretic fuzzy clustering algorithm for image segmentation. *Comput Vis Image Underst* 2013;117(10):1412–20.
- [20] Caldaïrou B, Passat N, Habas PA, Studholme C, Rousseau F. A non-local fuzzy segmentation method: application to brain MRI. *Pattern Recogn* 2011;44(9):1916–27.
- [21] Zhao F, Jiao L, Liu H. Fuzzy c-means clustering with non local spatial information for noisy image segmentation. *Front Comput Sci China* 2011;5(1):45–56.
- [22] Ji Z-X, Sun Q-S, Xia D-S. A modified possibilistic fuzzy c-means clustering algorithm for bias field estimation and segmentation of brain mr image. *Comput Med Imaging Graph* 2011;35(5):383–97.
- [23] Chen C-M, Chen C-C, Wu M-C, Horng G, Wu H-C, Hsueh S-H, Ho H-Y. Automatic contrast enhancement of brain mr images using hierarchical correlation histogram analysis. *J Med Biol Eng* 2015;35(6):724–34.
- [24] Alipour S, Shanbehzadeh J. Fast automatic medical image segmentation based on spatial kernel fuzzy c-means on level set method. *Mach Vision Appl* 2014;25(6):1469–88.
- [25] Ali H, Elmogly M, El-Daydamony E, Atwan A. Multi-resolution MRI brain image segmentation based on morphological pyramid and fuzzy c-mean clustering. *Arab J Sci Eng* 2015;40(11):3173–85.
- [26] Deng W-Q, Li X-M, Gao X, Zhang C-M. A modified fuzzy c-means algorithm for brain mr image segmentation and bias field correction. *J Comput Sci Technol* 2016;31(3):501–11.
- [27] Bezdek JC. *Pattern recognition with fuzzy objective function algorithms*. Springer Science & Business Media; 2013.
- [28] Alruwaili M, Javed A, Javed MS. Hybrid genetic filter for restoration of brain MRI images corrupted with impulse noise. *Int J Comput Sci Network Secur (IJCSNS)* 2017;17(2):252.
- [29] Smith SM. Fast robust automated brain extraction. *Human Brain Mapping* 2002;17(3):143–55.
- [30] Dong Y, Xu S. A new directional weighted median filter for removal of random-valued impulse noise. *IEEE Signal Process Lett* 2007;14(3):193–6.
- [31] McAuliffe MJ, Lalonde FM, McGarry D, Gandler W, Csaky K, Trus BL. Medical image processing, analysis and visualization in clinical research. In:

- Proceedings 14th IEEE Symposium on Computer-Based Medical Systems. CBMS 2001. IEEE. p. 381–6.
- [32] Cma.mgh.harvard.edu.<http://www.cma.mgh.harvard.edu/ibsr/> [accessed: 2019-03-20].
- [33] Dice LR. Measures of the amount of ecologic association between species. *Ecology* 1945;26(3):297–302.
- [34] Shi R, Ngan KN, Li S, Paramesran R, Li H. Visual quality evaluation of image object segmentation: Subjective assessment and objective measure. *IEEE Trans Image Process* 2015;24(12):5033–45.
- [35] Thung K-H, Raveendran P. A survey of image quality measures, in, international conference for technical postgraduates (TECHPOS). IEEE 2009;2009:1–4.
- [36] Qiu C, Xiao J, Yu L, Han L, Iqbal MN. A modified interval type-2 fuzzy c-means algorithm with application in mr image segmentation. *Pattern Recogn Lett* 2013;34(12):1329–38.